Ricochet off water of spherical projectiles

Article *in* Journal of Ship Research · June 1991

CITATIONS
9

READS
137

1 author:

Touvia Miloh
Tel Aviv University
259 PUBLICATIONS **2,892** CITATIONS

SEE PROFILE

Journal of Ship Research, Vol. 35, No. 2, June 1991, pp. 91–100

Journal of
Ship Research

Ricochet Off Water of Spherical Projectiles[1]

T. Miloh[2] and **Y. Shukron**[3]

The oblique water-entry problem of a spherical projectile is analytically analyzed with special reference to the ricocheting phenomena of the object off a free surface. Under the assumption of large impact velocity, the Kelvin-Kirchoff-Lagrange equations of motion are formulated in terms of the various time-dependent added-mass coefficients and their time derivatives. The actual trajectory of the sphere below the free surface is obtained by integration of these equations, and a critical value for the projectile incident angle (ricochet) is obtained in terms of the initial Froude number and the specific density of the solid. It is demonstrated that for infintely large Froude numbers this solution reduces to the well-known empirical expression for the critical angle of a sphere in oblique water-entry.

Dedicated to Marshall Tulin on the occasion of his 65th birthday

Introduction

ONE OF THE fascinating problems in hydrodynamics is the ricocheting or bouncing of a rigid body (projectile) off a free surface. A ricochet may occur when the projectile hits the free surface at grazing angles with relatively large impact speed. The ricocheting phenomenon of spherical shapes is of particular interest, mainly because of its past maritime application of attacking surface ships with cannon balls. This particular naval gunnery technique has been known since the 18th century and was extensively used during the Battle of Trafalgar (see historical account on the subject by Johnson and Reid [1][4]). However, the ricochet method is most well known for its use in breaching the Möhne Dam on the Ruhr by the RAF 617 squadron on the night of 14 May 1943 (project Downwood). This operation, as well as the air raid on two other dams on the same night, is associated with the name Barnes Wallis's "bouncing bomb" and is well documented in [2]. Today there is a renewed interest in the ricochet phenomena mainly in connection with flat oblique water-entry problems, water-landing of seaplanes and as a design criterion for protecting ocean sites against air-sea missiles. Finally, this phenomenon has always been a fascination and a challenge for each one of us, as we have all tried to make stones skip across the water surface by throwing them at small incident angles.

The hydrodynamical aspects of the ricochet phenomenon are very involved, and for these reasons analytic attempts for analyzing this problem hardly exist. Nevertheless, it is rather remarkable that there exists the following surprisingly simple empirical formula for the critical angle of entry θ_c of a sphere in terms of σ, which denotes the projectile specific density:

$$\theta_c = 18^0/\sqrt{\sigma} \tag{1}$$

Thus, if the water-entry angle of a spherical projectile is larger than θ_c, a ricochet will not occur and the heavy projectile will sink into the fluid. This empirical relationship was found to correlate quite well with experimental and field measurements of critical angles of high-speed spherical shapes. It is difficult to trace the origin of equation (1), which has been known, at least, since the turn of the century [1]. It is also well known that such a critical angle decreases with decreasing impact velocity until a threshold velocity is reached below which a ricochet is not possible. Such a speed-dependence effect is obviously not predicted by equation (1) which, for this purpose, may be considered only as an infinitely large Froude number asymptote. Here the Froude number is defined as $F_R^2 = W^2/gR$, where W denotes the impact velocity, g is the acceleration of gravity, and R represents the radius of the impinging solid sphere.

In spite of the relative simplicity of the empirical relationship (1), and its usefulness as a practical design criterion, there exist only very few reported attempts for providing analytical framework for (1). As far as we know the first analytical treatment of the ricochet problem of a sphere is due to Birkhoff et al [3], which appeared in a classified report. Birkhoff's original approach has been modified and re-represented by Johnson and Reid [1] and Hutchings [4]. These two works are similar in the sense that they are based on the following assumptions:

(*a*) A quasi-steady approach is assumed throughout the

[1]Preliminary results of this work were presented at the Fifth International Workshop on Water Waves and Floating Bodies, Manchester, England, March 25–28, 1990.

[2]Professor of Hydrodynamics, Department of Fluid Mechanics and Heat Transfer, Tel-Aviv University, Ramat-Aviv, Israel.

[3]Israel Aircraft Industry.

[4]Numbers in brackets designate References at end of paper.

Manuscript received at SNAME headquarters June 12, 1990; revised manuscript received December 6, 1990.

process and the velocity of the projectile remains constant during its encounter with the medium.

(*b*) Only the hydrodynamic pressure is responsible for the ricochet and the pressure is prescribed a priori over the wetted part of the sphere, in the form of

$$p = \frac{1}{2}\rho W^2 F(\beta) \tag{2}$$

where ρ is the fluid density, W the sphere velocity, and β the local angle between the projectile velocity vector and the normal to the surface of the sphere. Using a supersonic flow analogy, Johnson and Reid [1] and Birkhoff et al [3] make an ansatz that

$$F(\beta) = \cos^2\beta \tag{3}$$

On the other hand Hutchings [4] claims, by using Rayleigh's expression for the pressure distribution over a planing flat plate, that choosing

$$F(\beta) = \frac{2\pi\cos\beta}{4 + \pi\cos\beta} \tag{4}$$

is more appropriate for the present case than the Birkhoff's model (3). No physical reasons for using either pressure distributions (3) or (4) are given.

(*c*) The splash created on the forward side of the sphere (the so-called wetting correction) is altogether neglected in the treatments of references [1] and [3]. With reference to the notations of Fig. 1, this assumption implies that $\phi_w = \phi_0$ and that the instantaneous submerged portion of the sphere has a sector angle of $2\phi_0$. Hutchings [4], in an attempt to partially consider the effect of splash assumes $\phi_w = 2\phi_0$, again without providing any physical reasoning for this particular choice.

(*d*) In order to impose a realistic ricochet criterion, Birkhoff et al [3], followed by Johnson and Reid [1], claim that when the sphere is just *fully* submerged the normal velocity (in the direction of gravity) of the sphere must vanish. This condition is then used as a threshold criterion for the occurrence of critical ricochet. Hutchings [4], on the other hand, suggests that the proper critical condition is obtained when the normal velocity of the sphere vanishes at the instant where the sphere is exactly *half* submerged below the undisturbed free surface. Again, no explanation or proof is supplied for this particular choice.

In studying the above-mentioned works it was hard for us to understand some of the hydrodynamical assumptions, made on an ad hoc basis in the course of the analysis, which seem to lack in physical rigor. In particular, we were puzzled by the physical justification for selecting the particular pressure distribution (*b*) and by the theoretical basis for using the ricochet criterion employed in (*d*). Enchanted by the simplicity and the common applicability of equation (1) on one hand, and intrigued by its theoretical origin and the missing Froude number dependence [not predicted by (1)], we have decided to take a fresh look at this classical problem.

The present theoretical approach is based on applying an energy method and employs the Kelvin-Kirchhoff equations of motion, rather than on pressure integration. This method involves the temporal evaluation of the various added-mass coefficients and their time-derivatives in the high-frequency limit by ignoring the spray energy with respect to the total fluid kinetic energy. Thus, there is no need to assume a prescribed pressure distribution over the spherical surface, as in (*b*). Also employed here is what is believed to be a more realistic ricochet criterion which states that criticality is achieved when, during water-exit phase, the sphere is just above the undisturbed free surface and has *zero* normal velocity (see Fig. 2). Using this critical ricochet condition implies that the maximum penetration of the sphere is found from the complete solution of the problem and need not be defined a priori, as in (*d*). Indeed, as demonstrated in the sequel, the maximum penetration of the sphere below the undisturbed free surface, here denoted by b_{max} (Fig. 1), depends on the Froude number and is generally bounded by $R < b_{max} < 2R$, in agreement with the experimental data of Richardson [5]. The proposed analytical model also renders the trajectories of the submerged sphere and their variations with both Froude number and water-entry angle. Finally, the new model provides us with a theoretical framework for the origin of equation (1) and demonstrates that this empirical relationship is in fact the *infinite* Froude number asymptote of the analytic solution. In addition to determining the Froude number dependence of the critical angle, it is also possible to predict the minimum Froude number below which a ricochet will not occur, no matter how small is the incident angle.

Analysis

Before embarking on the complete solution of the ricochet problem it is convenient first to discuss some simplified cases which involve the motion of a rigid sphere toward or parallel to a free surface. In these two auxiliary problems the effect of gravity is ignored with respect to inertia, and the free surface is replaced by a flat equipotential surface. This assumption corresponds to the large-impact approximation often made in water-entry problems (Greenhow and Yanabo [6], Korobkin and Pukhnachov [7] and Korobkin [8]), following the classical contributions of Von Karman [9], Wagner [10], and Sedov [11].

Thus, we consider a rigid sphere of radius R, initially at rest, which is submerged to a depth of b below a free surface in a quiescent fluid (Fig. 1). At a certain instance (say $t = 0$), an impulsive velocity W ($W^2 = U^2 + V^2$) is imparted to the sphere where U and V denote the horizontal (sway) and

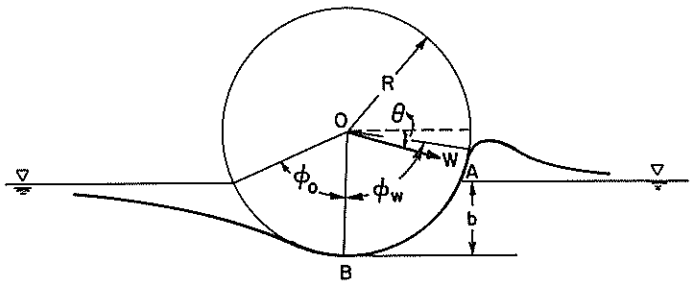

Fig. 1 Oblique water entry: definition sketch

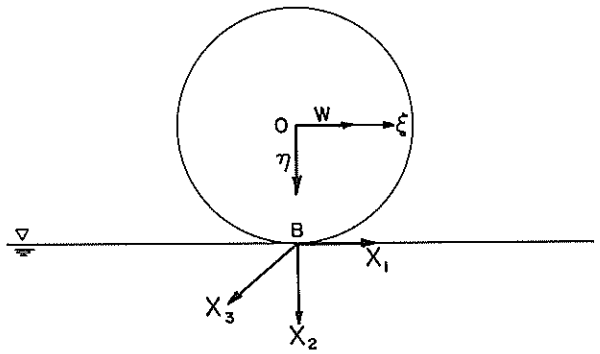

Fig. 2 Ricochet criterion at water exit

vertical (heave) velocity components. A typical velocity of a water-entry projectile (few inches in diameter) is usually of the order of 100 fps (Richardson [5]) which implies that the Froude number, $F_R^2 = W^2/gR$, is relatively large and is of the order of a few hundreds. Thus, viscous and surface tension effects may be ignored with respect to inertia and the flow may be assumed to be irrotational. Assuming that $U = \dot{X}_1$ and $V = \dot{X}_2$ are some slowly varying functions of time, a quasi-steady approach suggests that the total velocity potential may be decomposed into

$$\Phi(\mathbf{X},t) = \dot{X}_1(t)\Phi_1(\mathbf{X}) + \dot{X}_2(t)\Phi_2(\mathbf{X}) \tag{5}$$

where Φ_1 and Φ_2 denote the Kirchoff's unit velocity potentials in the horizontal and vertical directions respectively. Here $\mathbf{X}(X_1,X_2,X_3)$ represent a Cartesian coordinate system with an origin at the undisturbed free surface, with X_2 pointing downward in the direction of gravity (Fig. 2). The general boundary-value problem has been formulated in Miloh [12], and here we reproduce only the linearized version of the complete solution which is used in the subsequent analysis. Thus for $i = 1,2$ one gets

$$\begin{aligned} &\nabla^2\Phi_i = 0 \quad \text{in } \mathcal{V} \\ &\Phi_i = 0 \quad \text{on } X_2 = 0 \\ &\frac{\partial\Phi_i}{\partial n} = \frac{\partial x_i}{\partial n} \quad \text{on } S \\ &|\nabla\Phi_i| \to 0 \quad \text{as} \sum_{j=1}^{3} X_j^2 \to \infty \end{aligned} \tag{6}$$

where $\mathcal{V}$ denotes the volume of the fluid exterior to the sphere, S is the wetted surface of the sphere and n represents the outward normal. Once equation (6) is solved for the Kirchoff potentials, it is possible to define the various added-mass coefficients as

$$C_i(\tau) = \frac{1}{\pi R^3}\int_S \Phi_i \frac{\partial\Phi_i}{\partial n}\,dS \quad i = 1,2 \tag{7}$$

where $\tau = b/R$ is the instantaneous dimensionless submergence depth. These coefficients are related to the total kinetic energy T of the fluid (of density ρ) induced by the motion of the sphere

$$T = \frac{1}{2}\pi\rho R^3[C_1(\tau)\dot{X}_1^2 + C_2(\tau)\dot{X}_2^2] \tag{8}$$

Finally, for this particular case, the hydrodynamical loads experienced by the sphere may be simply obtained from the Lagrange equations of motion (Lamb [13] pp. 187–192), that is

$$\begin{aligned} F_1 &= -\frac{d}{dt}\left(\frac{\partial T}{\partial \dot{X}_1}\right) \\ &= -\pi\rho R^3 C_1(\tau)\ddot{X}_1 - \pi\rho R^2 D_1(\tau)\dot{X}_1\dot{X}_2 \\ F_2 &= -\frac{d}{dt}\left(\frac{\partial T}{\partial \dot{X}_2}\right) + \frac{\partial T}{\partial X_2} \\ &= -\pi\rho R^3 C_2(\tau)\ddot{X}_2 + \frac{1}{2}\pi\rho R^2[D_1(\tau)\dot{X}_1^2 - D_2(\tau)\dot{X}_2^2] \end{aligned} \tag{9}$$

The various (heave and sway) added-mass coefficients $C_i(\tau)$ and the corresponding so-called slamming coefficients

$$D_i(\tau) = \frac{dC_i(\tau)}{d\tau} \quad (i = 1,2)$$

for a partially submerged sphere have been computed in Miloh [12]. The formulation is based on expansion of the velocity potentials in terms of toroidal harmonics and use of the Mehler-Fock integral transform. The analytic procedure for determining these coefficients is rather involved and here we chose to represent only the final expressions for the added-mass coefficients: The "heave" added-mass $C_2(\tau)$ is given by

$$C_2(\tau) = \frac{2}{3}\sin^3\theta_0 \int_0^\infty (4p^2+1)[3tghp\theta_0 - tghp(\pi-\theta_0)] \cdot \frac{\cosh^2 p(\pi-\theta_0)}{\sinh(2p\pi)}\,dp \tag{10}$$

where

$$\theta_0 = \cos^{-1}(\tau - 1) \tag{11}$$

The "sway" added-mass is obtained from

$$C_1(\tau) = \frac{\sqrt{2}}{3}\sin^3\theta_0 \int_0^\infty (4p^2+1)A(p;\theta_0)tghp\theta_0 \cdot \frac{\sinh p(\pi-\theta_0)}{\sinh p\pi}\,dp \tag{12}$$

where $A(p;\theta_0)$ is found by solving the following Fredholm integral equation of the second kind

$$A(p;\theta_0) + \frac{1}{2}\sin\theta_0 tghp\pi \int_0^\infty A(q;\theta_0)I(p,q;\theta_0)tghq\theta_0 dq = \frac{4\sqrt{2}}{3}\frac{\sinh p(\pi-\theta_0)}{\cosh p\pi} \tag{13}$$

The kernel of equation (13) is defined as

$$I(p,q;\theta_0) = \int_1^\infty \frac{P_{-1/2+pi}(\mu)P_{-1/2+qi}(\mu)}{x - \cos\theta_0}\,d\mu \tag{14}$$

where $P_r(x)$ denotes the Legendre polynomial of order r (a complex number in the present case). The slamming coefficients are next obtained by differentiating equations (10) and (12) with respect to τ. The final solution for both $C_i(\tau)$ and $D_i(\tau)(i = 1,2)$ is plotted in Figs. 3–6.

The next step is to incorporate the hydrodynamical reactions of equation (9) into the full equations of motion which govern the time-dependent motion of the sphere through the fluid. It is assumed, following Johnson and Reid [1], that the forward attachment point of the free surface on the sphere (point A in Fig. 7), is at the undisturbed free-surface level. The rear reattachment point B is located on a limiting tangential streamline (Birkhoff and Caywood [14]), such that the sphere velocity vector is perpendicular to the radius vector $\overline{OB}$. In this configuration, the instantaneous submergence depth τ is defined as $\overline{CD}$ where $\overline{OD} \perp \overline{AB}$. We now define a new 2-D Cartesian coordinate system (x_1,x_2) centered at C, such that x_1 lies in the direction of AB and x_2 is normal to it as depicted in Fig. 7. The "lift" (F_2) and "drag" (F_1) hydrodynamical forces experienced by the sphere are then given by equation (9), where $\dot{X}_1$ and $\dot{X}_2$ denote now the components of the velocity vector along the x_1 and x_2 direction respectively. In addition to the body-fixed coordinate system (x_1,x_2), it is also advantageous to define an inertial system (ξ,η) centered at 0 such that η is aligned in the direction of gravity (Fig. 7). Let us also denote the total hydrodynamical forces acting in the ξ- and η-directions by F_h (horizontal) and F_v (vertical) respectively. It is possible then to express the

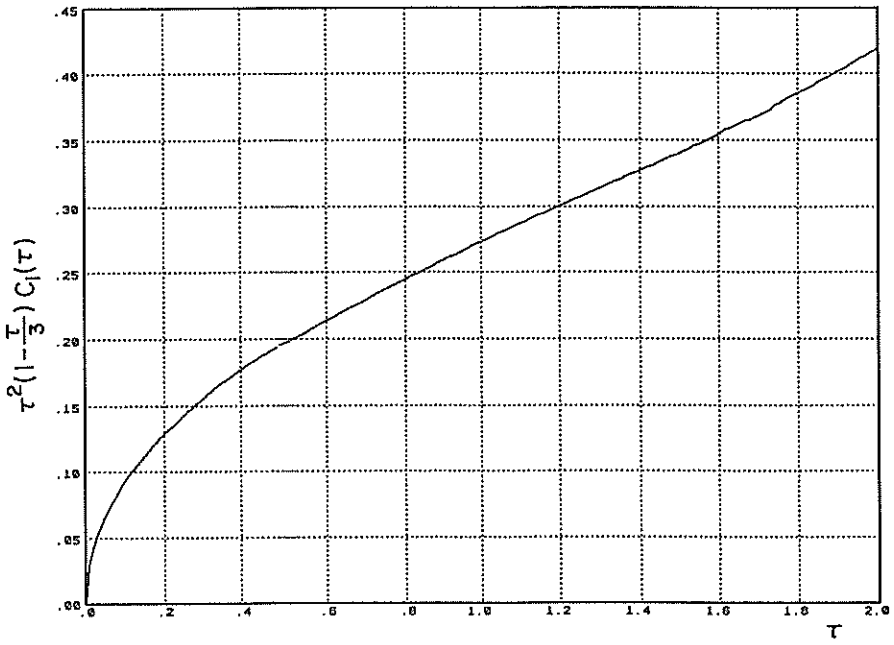

Fig. 3 Horizontal added-mass coefficient versus depth of submergence

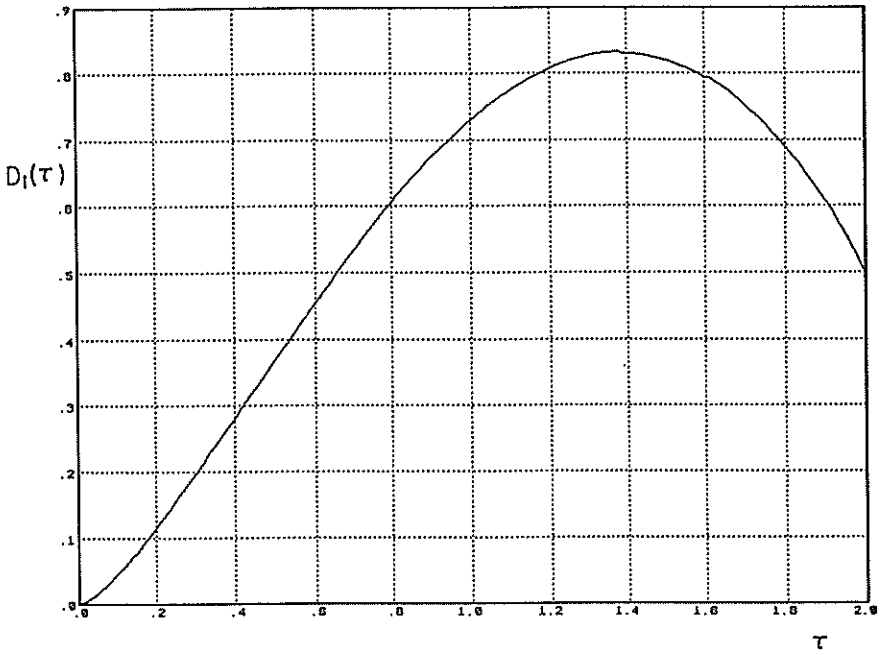

Fig. 4 Horizontal slamming coefficient versus depth of submergence

body equations of motion as

$$M\ddot{\xi} = F_h \quad ; \quad M\ddot{\eta} = Mg - B + F_v \tag{15}$$

where M is the body mass and B represents the buoyancy, given in terms of the body radius R and the dimensionless submergence τ as

$$B = \frac{1}{3}\rho g\pi R^3\tau^2(3-\tau) \tag{16}$$

In order to establish the relationship between the force components (F_h,F_v), measured in the inertial system and (F_1,F_2) which are defined in the body-fixed system, we denote the instantaneous angle between the two coordinate systems by ψ (see Fig. 7). Thus, the various velocity components are related by

$$\dot{x}_1 = \dot{\xi}\cos\psi - \dot{\eta}\sin\psi$$
$$\dot{x}_2 = \dot{\xi}\sin\psi + \dot{\eta}\cos\psi \tag{17}$$

Denoting the instantaneous elevation of the sphere center above the undisturbed free-surface level by η_0 one gets

$$\psi = \frac{1}{2}\cos^{-1}(\eta_0/R) - \frac{1}{2}\theta \tag{18}$$

and the dimensionless effective depth, $\tau = \overline{CD}/R$, is

$$\tau = 1 - \cos\left\{\frac{1}{2}\cos^{-1}(\eta_0/R) + \frac{1}{2}\theta\right\} \tag{19}$$

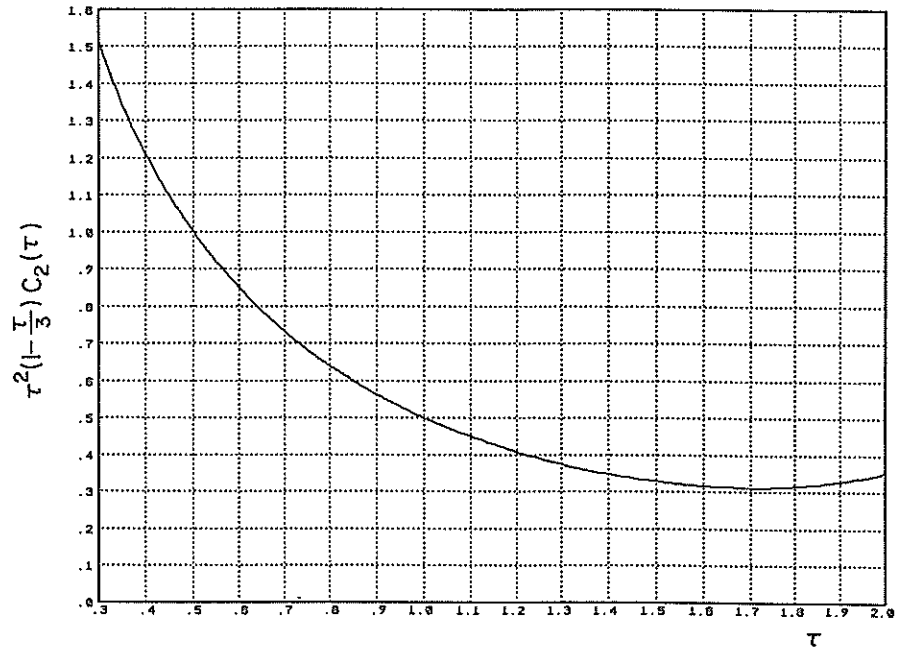

Fig. 5 Vertical added-mass coefficient versus depth of submergence

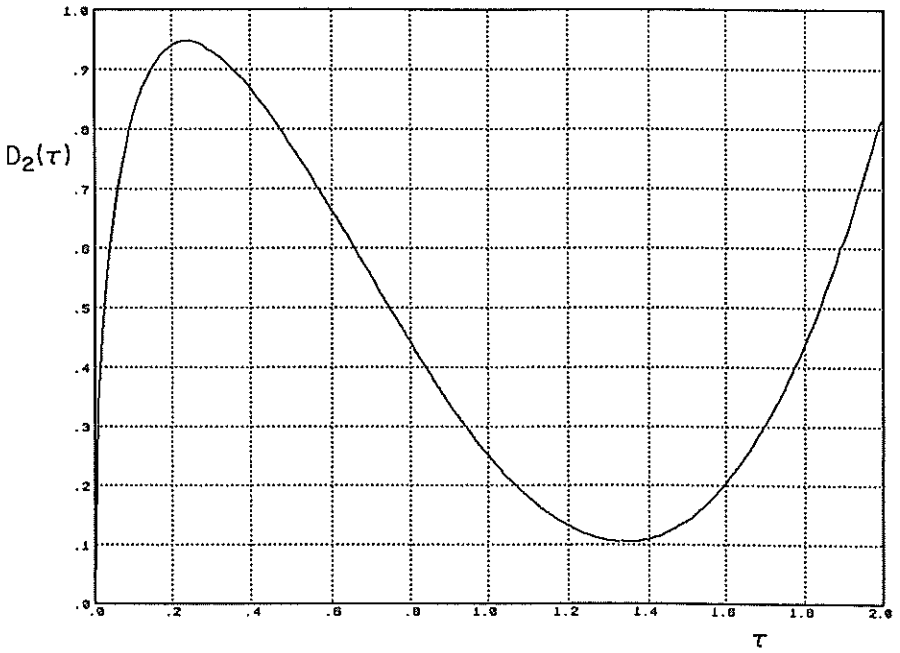

Fig. 6 Vertical slamming coefficient versus depth of submergence

where θ is the so-called "angle of attack" (the angle between the sphere velocity vector and the horizontal direction) that is

$$\theta = tg^{-1}(\dot{\eta}/\dot{\xi}) \tag{20}$$

Next we substitute (17) in (9) and note that

$$F_h = F_1 \cos\psi + F_2 \sin\psi$$
$$F_v = -F_1 \sin\psi + F_2 \cos\psi \tag{21}$$

Thus, the horizontal and vertical components of the hydrodynamical force in equation (15) are expressible in terms of both the centroid velocity $(\dot{\xi},\dot{\eta})$, and acceleration $(\ddot{\xi},\ddot{\eta})$ vectors as well as the instantaneous submergence η_0.

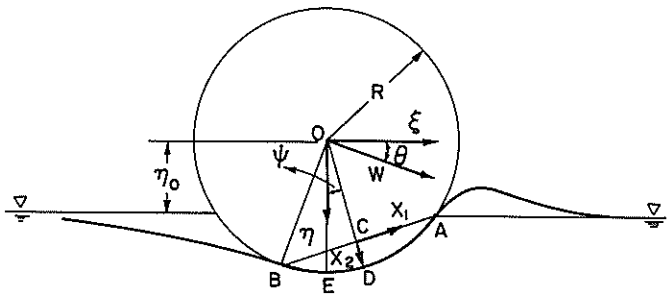

Fig. 7 Body-fixed and inertial coordinate systems

Finally, the substitution of equations (9), (16), (17) and (21) in (15), renders the following dimensionless expressions for the acceleration vector

$$\begin{pmatrix}\ddot{\xi}\\ \ddot{\eta}\end{pmatrix} = \begin{pmatrix}\alpha\\ \beta\end{pmatrix}\left[\frac{4\sigma}{3} + C_1(\tau)\cos^2\psi + C_2(\tau)\sin^2\psi\right] - \begin{pmatrix}\beta\\ \alpha\end{pmatrix}[C_2(\tau) - C_1(\tau)] \quad (22)$$

where in normalizing (22), R and R/W were used as characteristic length and time scales respectively (W being the total velocity at first impact). The nondimensional quantities which appear in (22) are defined below in terms of the added-mass $C_i(\tau)$ and slamming coefficients $D_i(\tau) = [dC_i(\tau)]/d\tau$, such as

$$\alpha(\dot{\xi},\dot{\eta},\tau) = \frac{1}{\gamma}[-D_1(\tau)\cos\psi(\dot{\xi}\cos\psi - \dot{\eta}\sin\psi)(\dot{\xi}\sin\psi + \dot{\eta}\cos\psi) + \frac{1}{2}D_1(\tau)\sin\psi(\dot{\xi}\cos\psi - \dot{\eta}\sin\psi)^2 - \frac{1}{2}D_2(\tau)\sin\psi(\dot{\xi}\sin\psi + \dot{\eta}\cos\psi)^2] \quad (23)$$

$$\beta(\dot{\xi},\dot{\eta},\tau) = \frac{1}{\gamma}\left[\frac{4\sigma}{3F_R^2} - \frac{\tau^2(3-\tau)}{3F_R^2} + D_1(\tau)\sin\psi(\dot{\xi}\cos\psi - \dot{\eta}\sin\psi)(\dot{\xi}\sin\psi + \dot{\eta}\cos\psi) + \frac{1}{2}D_1(\tau)\cos\psi(\dot{\xi}\cos\psi - \dot{\eta}\sin\psi)^2 - \frac{1}{2}D_2(\tau)\cos\psi(\dot{\xi}\sin\psi + \dot{\eta}\cos\psi)^2\right] \quad (24)$$

where

$$\gamma = \left(\frac{4\sigma}{3} + C_1(\tau)\cos^2\psi + C_2(\tau)\sin^2\psi\right)\cdot\left(\frac{4\sigma}{3} + C_1(\tau)\sin^2\psi + C_2(\tau)\cos^2\psi\right) - [C_2(\tau) - C_1(\tau)]^2 \quad (25)$$

Here, again $F_R^2 = W^2/gR$ denotes the reference Froude number at the instant of impact and σ, as before, represents the sphere specific density. It is important to note, following (19) and (20), that the angle ψ between the two Cartesian coordinate systems in Fig. 7, depends also on the instantaneous velocity vector $(\dot{\xi},\dot{\eta})$ and on the submergence τ. The time derivative of η_0, on the other hand, is simply equal to $\dot{\eta}$. Thus, using the dimensionless time t as a parameter, equation (22) may be integrated twice to render the actual trajectory $(\xi(t),\eta(t))$, of the sphere centroid during its submerged phase following the oblique water impact. With reference to Fig. 7 it is noted that initially ($t = 0$) one has

$$\xi(0) = 0\ ;\ \eta(0) = 1$$
$$\dot{\xi}(0) = \cos\theta_0\ ;\ \dot{\eta}(0) = \sin\theta_0 \quad (26)$$

where θ_0 denotes the angle of incidence at impact. The physical trajectory of the sphere may then be determined by integrating equation (22) in terms of the three parameters; θ_0, F_R and σ. In particular, the critical (smallest) angle of incidence $\theta_0 = \theta_c$, which leads to a ricochet is obtained by requiring that as the sphere exits the free surface ($t = t_f$) it should acquire *zero* normal velocity, that is

$$\eta(t_f) = 1\ ;\ \dot{\eta}(t_f) = 0\ ;\ \ddot{\eta}(t_f) > 0 \quad (27)$$

Using this new "ricochet criterion" (27), the nonlinear ODE (22) is solved numerically using the so-called "shooting method," thus leading to the desired relationship $\theta_c(\sigma,F_R)$ for the critical angle. In addition, the total plough $\xi(t_f)$, the exit velocity $\dot{\xi}(t_f)$, the maximum penetration depth b_{max}, and other important parameters may also be determined by the same procedure in terms of the flow parameters, σ, F_R and θ_0.

Results and discussion

One of the main results of this paper is the establishment of the relationship between the critical angle θ_c and the flow parameters σ and F_R and the comparison of this analytical solution with the commonly used empirical formula (1). In order to calculate θ_c it was necessary first to specify what is actually meant by a "ricochet." We thought that a proper way of defining this critical condition is by the requirement that the sphere will emerge from the free surface with zero normal velocity (Fig. 2). Such a ricochet criterion is believed to be more realistic than the corresponding criteria, employed, for example, by Johnson and Reid [1] or Hutchings [4], namely that the normal velocity vanishes at the instant when the sphere is fully or half submerged below the undisturbed free surface respectively. The reason is that the later requirements are not sufficient to guarantee that the sphere will actually emerge from the water. Hence, the presently employed critical condition is believed to be a genuine ricochet criterion in the sense that it clearly distinguishes between cases where the sphere is able to bounce from the free surface (and actually leave it), due to the induced hydrodynamical lift, and cases where the sphere will always remain partially or fully submerged below the free surface.

A numerical procedure for integrating the equations of motion (15), in order to find the submerged trajectory of the sphere after the oblique water entry, has been presented in the previous section. The analysis is based on the assumption of large impact speed, which suggests that, at least in the free-surface boundary conditions, gravity effects may be neglected with respect to inertia and for this reason the free surface may be approximated by a flat equipotential surface. Bearing this in mind, it is possible to determine analytically the two time-dependent added-mass $C_i(\tau)$ coefficients (corresponding to heave and sway motions) and their time derivatives $D_i(\tau)$, which represent the slamming coefficients. These coefficients were calculated in Miloh [12] and are plotted versus the dimensionless submergence depth τ in Figs. 3–6. Substituting these values in equations (23–25) enables us to integrate (22) twice with respect to time and by using the "ricochet criterion" of equations (26–27) one obtains the sought relationship $\theta_c(\sigma,F_R)$.

A plot of the resulting dependence between the critical angle θ_c, the density ratio σ, and Froude number F_R is presented in Fig. 8. For a prescribed Froude number the critical angle always decreases with increasing density ratio σ. For a given density ratio the critical angle was found to slightly increase with increasing Froude number reaching a maximum value on an asymptote, which corresponds to infinite Froude number ($F_R \to \infty$). It is also interesting to note from the same figure that there exists a minimum Froude number below which a ricochet is not possible. Thus, actual values of critical angle always lie below (to the left) of the infinite Froude number asymptote and above (to the right) of the minimum Froude number asymptote (Figs. 8 and 10).

A very interesting observation can be made when replotting Fig. 8 on a new scale representing the variation of the product $\sqrt{\sigma}\,\theta_c$ versus σ for various Froude numbers (see Fig. 9). The striking observation in this case is that on the upper asymptote ($F_R \to \infty$) we obtain $\sqrt{\sigma}\,\theta_c \cong 18^0$, which is in surprisingly good agreement with the empirical relationship (1).

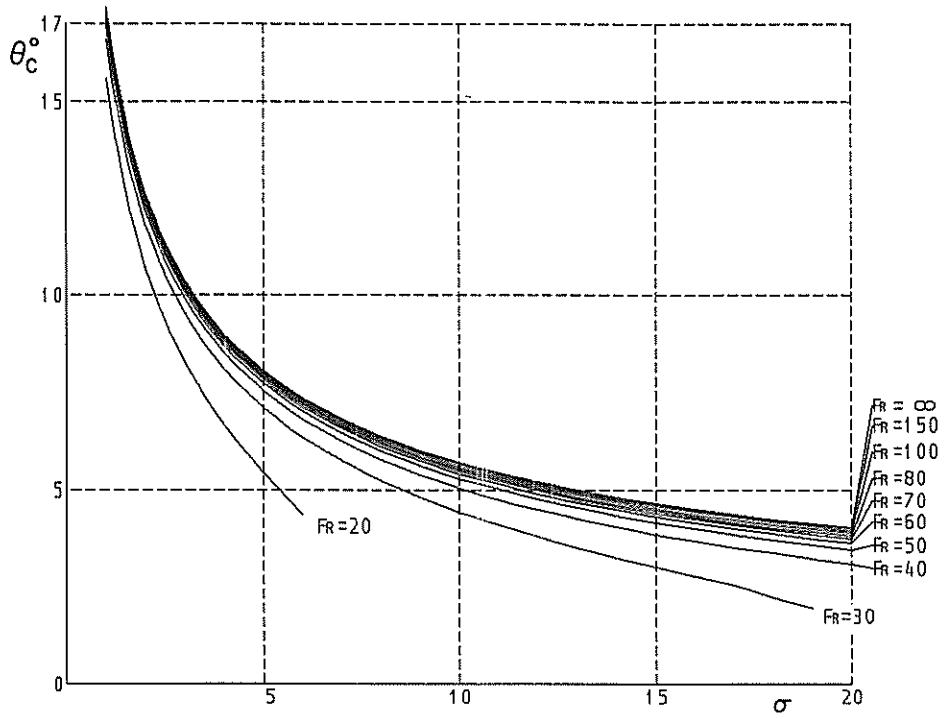

Fig. 8 Variation of critical angle with sphere specific density

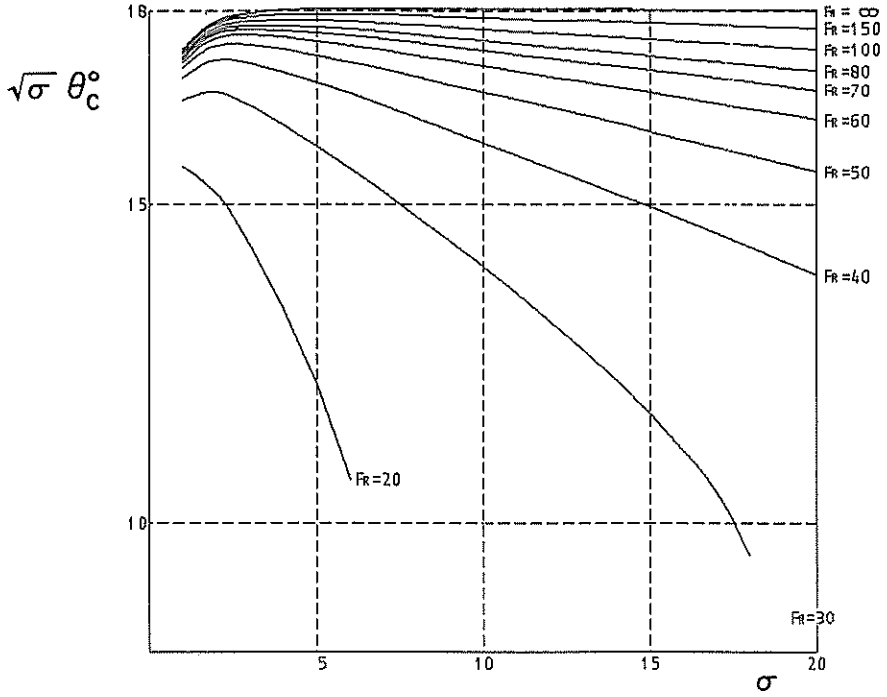

Fig. 9 Product $\sqrt{\sigma}\ \theta_c^0$ versus σ

Thus, it is claimed here that the present analysis provides some theoretical framework for the empirical relationship (1), which already has been known for some time, and suggests that (1) is in fact an upper bound for θ_c which corresponds to $F_R \to \infty$. For finite Froude numbers Fig. 9 shows a strong dependence of the product $\sqrt{\sigma}\theta_c$ on the Froude number.

A careful analysis of the variation of the minimum Froude number, below which a ricochet is not possible, resulted in Fig. 10. The numerical solution is also compared against the empirical relationship suggested by Soliman et al [15] for the lowest possible value of the critical impact angle, which implies that the minimum Froude number is bounded from below by

$$(F_R)_{\min} > \frac{20}{\pi}\sqrt{\sigma} \tag{28}$$

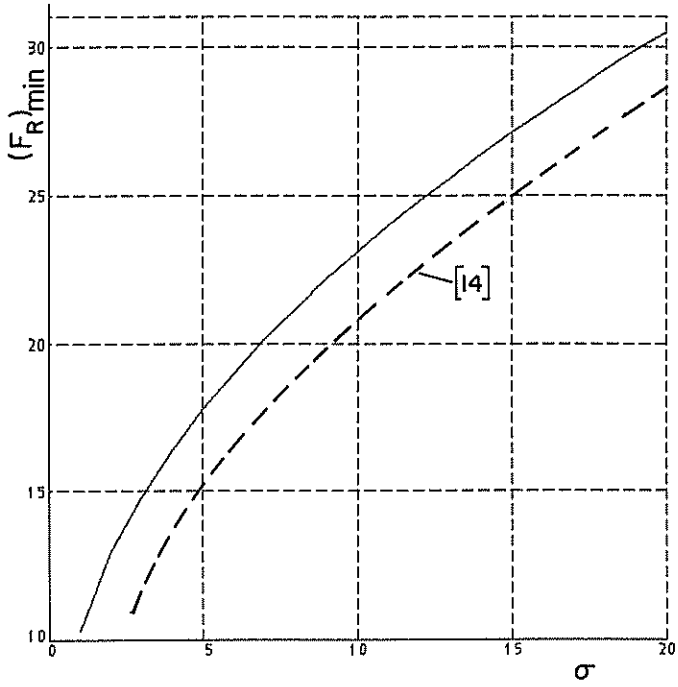

Fig. 10 Minimum Froude number versus σ and lower bound of [15]

Still another important parameter, which is obtained from the present analysis, is the maximum penetration depth of the sphere below the undisturbed free surface at critical (ricochet) water-entry conditions. The maximum depth is depicted in Fig. 11 in terms of the Froude number F_R and the density ratio σ. It is thus found that the maximum penetration b_{max} increases with Froude number (for a prescribed σ), but it does not exceed $1.4R$ even for infinitely large Froude numbers, and hardly falls below $0.9R$ at relatively small Froude numbers. This conclusion is also in agreement with the reported experimental findings of Richardson [5], where the maximum depth was found to vary between R and $2R$. It should also be noted that in the present method, unlike the approximate solutions proposed by Johnson and Reid [1] and Hutchings [4], there is no need to *fix a priori* the maximum depth which is found here as part of the general solution. Again, the reader is reminded that in [1] the maximum depth is arrested and is chosen to be the diameter, whereas in [4] it is taken as the radius, irrespective of the Froude number and density ratio.

As already mentioned, there hardly exists any experimental measurements of the critical angle versus Froude number for a particular value of σ. Maybe the only reported results are those of Soliman et al [15], where a steel sphere (σ = 7.8), 1 in. in diameter, was fired over a range of speeds between 20 and 250 fps and for each speed the critical angle θ_c has been determined from the initial setting of the gun. These experimental results are also presented in a dimensionless form in Fig. 12 as a plot of the critical angle θ_c with the initial Froude number. The agreement between the experimental results and the theoretical solution found in this study for σ = 7.8 (steel) is again surprisingly good. Also presented in the same figure is the variation of θ_c versus F_R for aluminium (σ = 2.7).

In addition to finding the critical angle of incidence θ_c, the present analysis is also capable of producing the precise trajectories of the sphere from the instant of water entry to water exit for arbitrary entry angles. The numerical scheme employed in this case for solving (22), is similar in essence to the one used to determine the critical angle θ_c. The only difference is in the initial conditions (26), where now θ_0 is prescribed as the entry angle and the end condition (27) becomes redundant. The numerical solution of the equations of motion (22) renders the trajectory of the sphere-centroid under the free surface in the form of $(x_1(t),x_2(t))$ as a function of the entry angle. Typical curves, representing the vertical

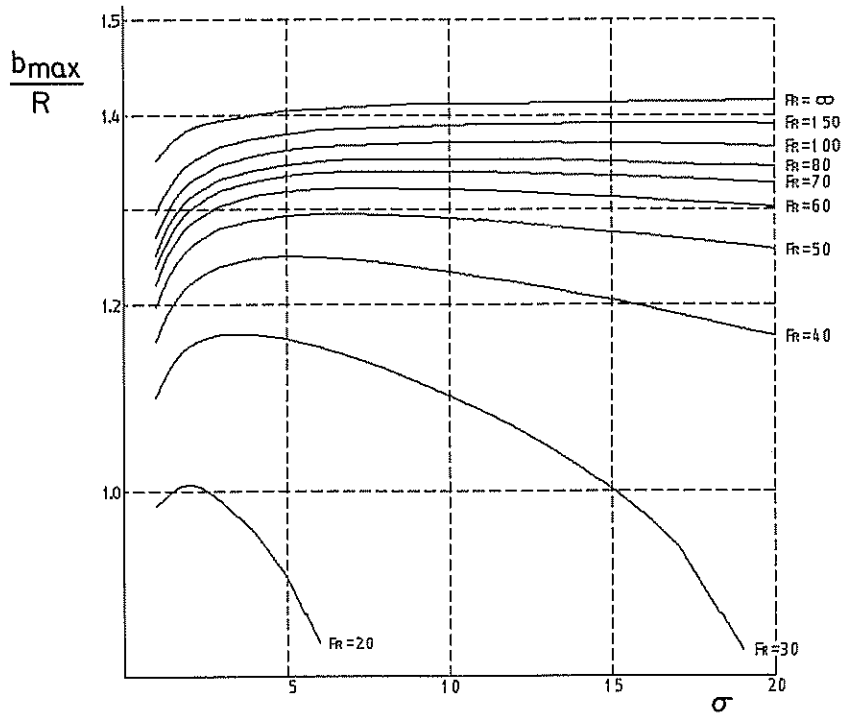

Fig. 11 Maximum penetration for critical conditions versus F_R and σ

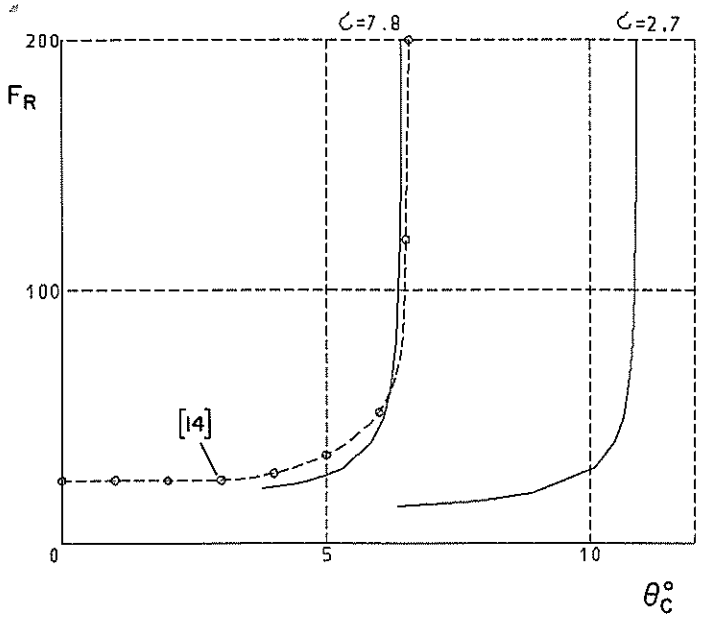

Fig. 12 Variation of θ_c with F_R for aluminium (σ = 2.7) and steel (σ = 7.8), against experimental data of [15]

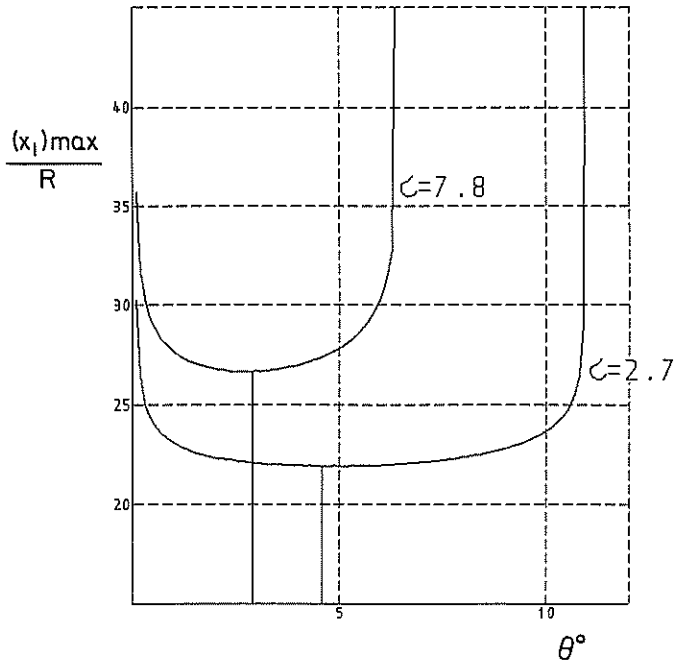

Fig. 15 Variation of horizontal plough with incident angles

coordinate x_2 in terms of the horizontal one x_1 for both σ = 2.7 (aluminium) and σ = 7.8 (steel) are depicted in Figs. 13 and 14 for several incidence angles. The maximum theoretical plough (ignoring viscous effects) for aluminium is smaller by almost a factor of 2 than the one corresponding to steel. The maximum plough is always obtained at $\theta_0 = \theta_c$, that is, at the critical angle; however, the minimum plough is achieved at some intermediate values, $0 < \theta_0 < \theta_c$, as demonstrated in Fig. 15.

The relationship between the entry angle θ_{in} and the exit angle θ_{out}, may also be explored using the proposed method and it is shown both for aluminium and steel that $\theta_{out} < \theta_{in}$ (Fig. 16). Finally, it is demonstrated that the exit velocity W_{out} is always smaller than the entry velocity W_{in} and their ratio clearly tends to zero as the entry-angle approaches the critical angle (Fig. 17). It is important to note that in the approximate models of [1] and [4], the horizontal component of the velocity was assumed to be constant. In our modified model, this assumption was proven to be faulty and a con-

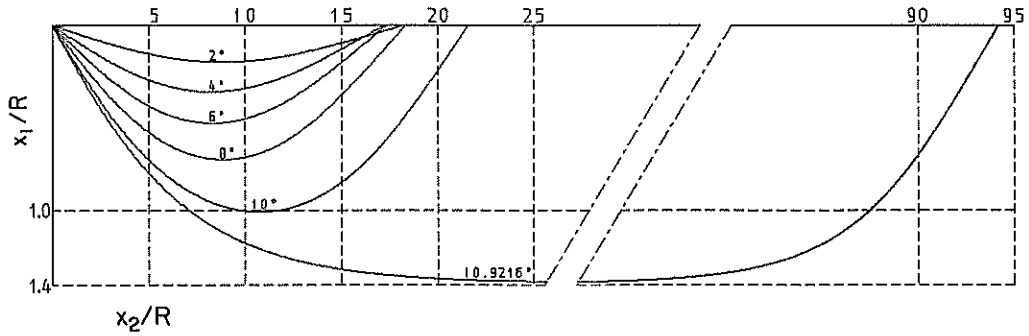

Fig. 13 Submerged trajectories for σ = 2.7 for various incident angles

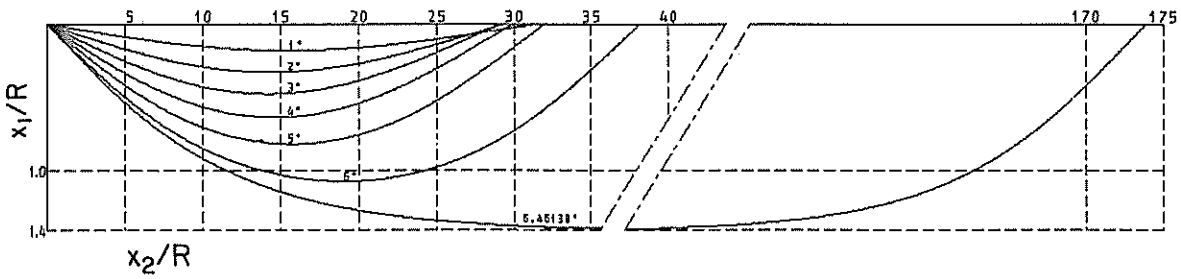

Fig. 14 Submerged trajectories for σ = 7.8 for various incident angles

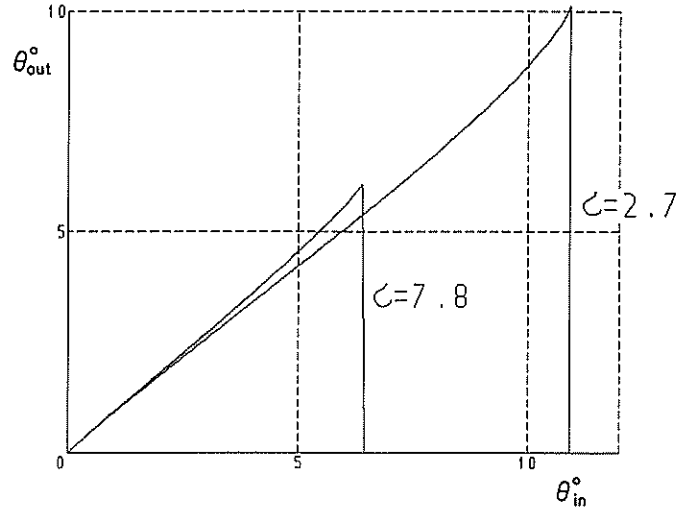

Fig. 16 Angle of incident versus exit angle

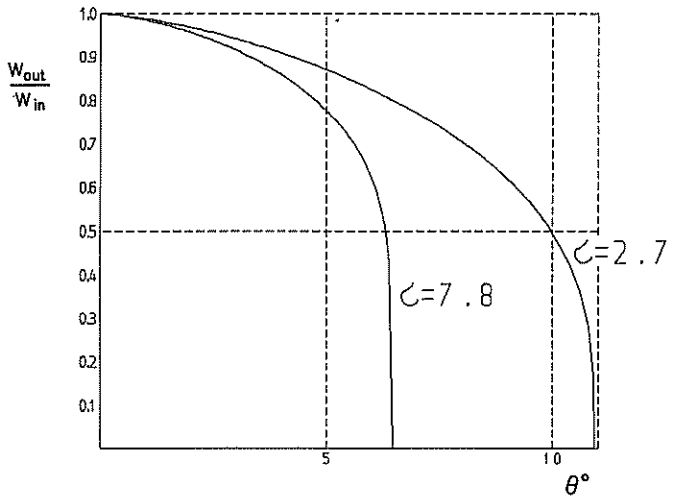

Fig. 17 Ratio between entry and exit velocities for various incident angles

siderable reduction in the horizontal velocity was obtained, even when viscous effects were ignored. As far as viscous effects are concerned, an attempt to incorporate such effects in the equations of motion (15), by including a standard quadratic drag term with a drag coefficient of about 0.4, did not seem to produce any significant change in the results, especially for large F_R. The reason is that for large Froude numbers (where ricocheting occurs) viscous effects may be usually neglected with respect to inertia.

References

1 Johnson, W. and Reid, S. R., "Ricochet of Spheres Off Water," *Journal of Mechanical Engineering Science,* Vol. 17, No. 2, 1975, pp. 71–81.

2 Morpurgo, J. E., *Barnes Wallis,* Longmans, London, 1972.

3 Birkhoff, G., Birkhoff, G. D., Bleick, W. E., Handler, E. H., Murnaghan, F. D. and Smith, T. L. "Ricochet Off Water," Applied Mathematics Panel, National Defense Research Committee, Memo. 42, 4M, AMG-C 1944.

4. Hutchings, I. A., "The Ricochet of Spheres and Cylinders from the Surface of Water," *International Journal of Mechanical Engineering Science,* Vol. 18, 1976, pp. 243–247.

5 Richardson, E. G., "The Impact of a Solid on a Liquid Surface" in *Proceedings,* Phys. Soc., Vol. 61, No. 4, 1948, pp. 352–367.

6 Greenhow, M. and Yanabo, L., "Added Mass for Circular Cylinders Near or Penetrating Fluid-Boundaries—Review, Extension and Application to Water Entry, Exit and Slamming," *Ocean Engineering,* Vol. 14, No. 4, 1987, pp. 325–348.

7 Korobkin, A. A. and Pukhnachov, V. V., "Initial Stage of Water Impact," *Annual Review of Fluid Mechanics,* Vol. 20, 1988, pp. 159–185.

8 Korobkin, A. A., "Inclined Entry of a Blunt Profile into an Ideal Fluid," *Fluid Dynamics,* Vol. 23, 1988, pp. 443–447.

9 Von Karman, Th., "The Impact on Seaplanes Floats During Landing," NACA TN 321, National Advisory Committee on Aeronautics, 1930.

10 Wagner, H., "Uber stoss und gleitvorgange an der oberflache von flussigbeiten," *Zeitschrift für Angewandte Mathematik und Mechanik,* Vol. 2, 1932, pp. 193–215.

11 Sedov, L., "The Impact of a Solid Body Floating on the Surface of an Incompressible Fluid," TSAGI Report, Works of the Central Aerodynamical Institute, No. 187, Moscow, 1934.

12 Miloh, T., "On the Oblique Water-Entry Problem of a Rigid Sphere," *Journal of Engineering Mathematics,* Vol. 25, 1991, pp. 77–92.

13 Lamb, H., *Hydrodynamics,* Dover, New York, 1932.

14 Birkhoff, G. and Caywood, T. E., "Fluid Flow Patterns," *Journal of Applied Physics,* Vol. 20, 1949, pp. 646–656.

15 Soliman, A. S., Reid, S. R. and Johnson, W., "The Effect of Spherical Projectiles Speed in Ricochet Off Water and Sand," *International Journal of Mechanical Science,* Vol. 18, 1976, pp. 279–284.